11-1-2017

Bimodal coupling of ripples and slower oscillations during sleep in patients with focal epilepsy.

Inkyung Song
Thomas Jefferson University

Iren Orosz
David Geffen School of Medicine at UCLA

Inna Chervoneva
Thomas Jefferson University

Zachary J. Waldman
Thomas Jefferson University

Itzhak Fried
David Geffen School of Medicine at UCLA

Authors

Inkyung Song, Iren Orosz, Inna Chervoneva, Zachary J. Waldman, Itzhak Fried, Chengyuan Wu, Ashwini Sharan, Noriko Salamon, Richard Gorniak, Sandra Dewar, Anatol Bragin, Jerome Engel, Michael R. Sperling, Richard Staba, and Shennan A. Weiss

Published in final edited form as:

Epilepsia. 2017 November ; 58(11): 1972–1984. doi:10.1111/epi.13912.

Bimodal coupling of ripples and slower oscillations during sleep in patients with focal epilepsy

Inkyung Song[1], **Iren Orosz**[2], **Inna Chervoneva**[3], **Zachary J. Waldman**[1], **Itzhak Fried**[4], **Chengyuan Wu**[5], **Ashwini Sharan**[5], **Noriko Salamon**[2], **Richard Gorniak**[6], **Sandra Dewar**[7], **Anatol Bragin**[7], **Jerome Engel Jr.**[7,8,9,10], **Michael R. Sperling**[1], **Richard Staba**[7], and **Shennan A. Weiss**[1]

[1]Dept. of Neurology, Thomas Jefferson University, Philadelphia, Pennsylvania, U.S.A. 19107

[2]Dept. of Radiology, David Geffen School of Medicine at UCLA, Los Angeles, California, U.S.A. 90095

[3]Dept. of Pharmacology & Experimental Therapeutics, Thomas Jefferson University, Philadelphia, Pennsylvania, U.S.A. 19107

[4]Dept. of Neurosurgery, David Geffen School of Medicine at UCLA, Los Angeles, California, U.S.A. 90095

[5]Dept. of Neurological Surgery, Thomas Jefferson University, Philadelphia, Pennsylvania, U.S.A. 19107

[6]Dept. of Radiology, Thomas Jefferson University, Philadelphia, Pennsylvania, U.S.A. 19107

[7]Dept. of Neurology, David Geffen School of Medicine at UCLA, Los Angeles, California, U.S.A. 90095

[8]Dept. of Neurobiology, David Geffen School of Medicine at UCLA, Los Angeles, California, U.S.A. 90095

[9]Dept. of Psychiatry and Biobehavioral Sciences, David Geffen School of Medicine at UCLA, Los Angeles, California, U.S.A. 90095

[10]Brain Research Institute, David Geffen School of Medicine at UCLA, Los Angeles, California, U.S.A. 90095

Summary

Objective—Differentiating pathological and physiological high-frequency oscillations (HFOs) is challenging. In patients with focal epilepsy, HFOs occur during the transitional periods between the up and down state of slow waves. The preferred phase angles of this form of phase-event

Corresponding author: Dr. Shennan A. Weiss, 900 Walnut Street, PA 19107, Phone: (215) 503-7960, Shennan.Weiss@jefferson.edu.

DR. ANATOL BRAGIN (Orcid ID: 0000-0003-1207-8481)

Disclosure of Conflicts of Interest

None of the authors has any conflict of interest to disclose.

Ethical Publication Statement

We confirm that we have read the Journal's position on issues involved in ethical publication and affirm that this report is consistent with those guidelines.

amplitude coupling are bimodally distributed, and the ripples (80–150 Hz) that occur during the up-down transition more often occur in the seizure onset zone (SOZ). We investigated if bimodal ripple coupling was also evident for faster sleep oscillations, and could identify the SOZ.

Methods—Using an automated ripple detector, we identified ripple events in 40–60 minute intracranial EEG (iEEG) recordings from 23 patients with medically refractory mesial temporal lobe or neocortical epilepsy. The detector quantified epochs of sleep oscillations and computed instantaneous phase. We utilized a ripple phasor transform, ripple-triggered averaging, and circular statistics to investigate phase event-amplitude coupling.

Results—We found that at some individual recording sites, ripple event amplitude was coupled with sleep oscillatory phase and the preferred phase angles exhibited two distinct clusters ($p<0.05$). The distribution of the pooled mean preferred phase angle, defined by combining the means from each cluster at each individual recording site, also exhibited two distinct clusters ($p<0.05$). Based on the range of preferred phase angles defined by these two clusters, we partitioned each ripple event at each recording site into two groups: depth iEEG peak-trough and trough-peak. The mean ripple rates of the two groups in the SOZ and NSOZ were compared. We found that in the frontal (spindle, $p=0.009$; theta, $p=0.006$, slow, $p=0.004$) and parietal lobe (theta, $p=0.007$, delta, $p=0.002$, slow, $p=0.001$) the SOZ incidence rate for the ripples occurring during the trough-peak transition was significantly increased.

Significance—Phase-event amplitude coupling between ripples and sleep oscillations may be useful to distinguish pathological and physiological events in patients with frontal and parietal SOZ.

Keywords

epilepsy; ripples; sleep oscillations; phase-event amplitude coupling; intracranial electroencephalography

Introduction

Features of seizures can differ depending on sleep stages as well as the location of seizure onset[1]. Temporal lobe seizures occur more frequently during wakefulness, but frontal and parietal lobe seizures occur more frequently during early non-rapid eye movement (NREM) sleep[2,3]. Accurate intracranial monitoring is often required when surgery is considered for patients with nocturnal seizures, especially those with the frontal lobe onset[4].

At least three cardinal oscillatory events of NREM sleep may contribute to the local and global neural changes that drive epileptogenesis: slow, spindle, and ripple oscillations[5]. Slow oscillations (~0.75 Hz) consisting of alternating phases of the hyperpolarized/down- and depolarized/up-state[6,7] involves cortical[8] and thalamic networks[9]. Spindle-band oscillations (12–16 Hz) are generated by smaller local networks of thalamic and cortical neurons, and are often phase-locked to slow oscillations during slow-wave sleep[10]. Ripples, defined as brief bursts (~50–150 msec) of high-frequency (80–200 Hz) neurophysiological activity, are highly synchronized local network events that occur concurrently with slow waves[11–14] and sleep spindles[13–15]. In humans with neocortical epilepsy, ripple rates can be increased primarily in the seizure-onset zone (SOZ), but sometimes also in the non-SOZ (NSOZ)[16].

Ripple events occur during both the transition between the down-up state, and the up-down state of slow waves. Thus, ripple amplitude can be considered coupled with slow wave phase at two preferred phase angles. The ripples coupled to one preferred phase angle (i.e., down-up state) may be physiological, and the ripples coupled to the other preferred phase angle (i.e., up-down state) may be pathological (Fig. 1). In accord with this notion, the ripple events that occur during the up-down transition are generated more frequently in the SOZ[5,17]. Also, intracranial EEG (iEEG) recordings from human hippocampus contralateral to the SOZ have demonstrated that ripple events that occur during the down-up transition are likely physiological because they are nested in the trough of spindle oscillations[13,14], and may mediate memory consolidation[18].

In principle, a method that can distinguish putative pathological from physiological ripples should be able to distinguish two clusters of ripple events. One of these clusters should exhibit elevated rates selectively in epileptogenic regions, relative to the other cluster. This technique was used to distinguish putative physiological and pathological ripples coupled with slow waves[5,17]. It is not yet clear if this method can be applied to ripples that occur superimposed on other sleep oscillations. To determine if coupling between ripple amplitude and the phase of delta, theta, and spindle sleep oscillations could help distinguish physiological ripple events from pathological ripple events, we 1) examined the relationship between the phase of the distinct oscillations composing core sleep architecture and the amplitude of ripple events, 2) defined two distinct populations of ripples based on the preferred phase angle of coupling, and 3) tested whether one of the populations had a higher incidence ratio in the SOZ (Fig. 1).

Methods

1. Patient selection

Recordings were selected from 18 patients with mesial temporal lobe, mesial temporal and neocortical (MTLE+), and neocortical focal epilepsy, who underwent intracranial monitoring with depth electrodes between 2014 and 2016 at University of California Los Angeles (UCLA), and five patients with neocortical epilepsy at Thomas Jefferson University (TJU) for the purpose of localization of the SOZ. The study was approved by the UCLA and TJU institutional review boards, and patients gave informed consent. Further information regarding inclusion criteria and neuroimaging studies and analysis is provided in the Supporting Information.

2. Intracranial EEG recordings and segment selection

Clinical iEEG sleep recordings (0.016–600 Hz; 2,000 samples per second) were acquired from 7–16 contact depth electrodes using a Nihon-Kohden 256-channel JE-120 long-term monitoring system (Nihon-Kohden America, Foothill Ranch, CA, USA) at UCLA and from 7–10 contact depth electrodes using the same amplifier at TJU (0.016–400 Hz; 1,000 samples per second) (Supporting information). For both UCLA and TJU iEEG data, a 40–90 min epoch of mixed-stage sleep was confirmed by video-EEG inspection revealing eyes closed, K-complexes, sleep spindles, epochs of high amplitude of slow and delta activity, and a paucity of muscle artifact[19].

3. Ripple detection and quantification

All iEEG recordings were imported from EDF format in to Matlab v2016b (Natick, MA, USA). Subsequent processing steps for those recordings from macroelectrodes deemed suitable on the basis of visual inspection using BESA v5 (Gräfelfing, Germany) were performed using custom software developed in Matlab. Muscle and electrode artifacts in iEEG recordings from were reduced using a custom independent component analysis (ICA)-based algorithm[20,21]. After applying this ICA-based method, ripples were detected in the referential montage iEEG recordings per contact by utilizing a Hilbert detector[20], in which (i) applied a 1000th order symmetric finite impulse response (FIR) band-pass filter (80–600 Hz), and (ii) applied Hilbert transform to calculate the instantaneous amplitude of this time series according to the analytic signal z(t), described in Eqn. 1.,

$$z(t) = a(t)\ e\hat{}i\phi(t) \quad \text{Eqn. 1}$$

where a(t) is the instantaneous amplitude and ø(t) is the instantaneous phase of z(t). Following the Hilbert transform, (iii) the instantaneous ripple amplitude function (a(t)) was smoothed using moving window averaging, (iv) the smoothed instantaneous ripple amplitude function was normalized using the mean and standard deviation of the time series, and (v) a threshold was used to detect the onset and offset of discrete/potential events (Supporting information).

4.1. Classifying ripples on spikes and lower-frequency oscillations during sleep—We used an established method to differentiate ripples on oscillations from ripples on spikes[20] (Supporting information). Ripples on spikes can arise due to Gibb's phenomenon as a result of high-pass filtering sharp transients, such as an epileptiform spike[22]. To distinguish authentic/true ripple events that occur during spikes from spurious/false ripple events due to filter ringing, we developed a custom algorithm using a topographic analysis of time-frequency plots[23] (Supporting information).

We categorized the ripple on oscillations in to subtypes using a novel approach. We first applied an optimized Hamming-windowed FIR band-pass filter (eegfiltnew.m; EEGLAB, https://sccn.ucsd.edu/eeglab) to all the iEEG recordings with the following low- and high-pass cutoff values: slow (0.1–2 Hz), delta (2–4 Hz), theta (4–10 Hz), and spindle band (12–16 Hz). We then calculated the instantaneous amplitude of the Hilbert transformed band-pass filtered signals (Eqn. 1). The instantaneous amplitude was normalized. For each distinct frequency band, we used different minimum amplitude and duration criteria to identify epochs in which oscillatory bursts appeared, this calibration was performed blinded to the results of the ripple analysis. The amplitude and duration thresholds for each oscillatory type were adjusted and optimized on the basis of visual inspection of computer annotated iEEG recordings. After identifying the epochs of slow, delta, theta-band, and spindle-band bursts, the time stamps were used to classify the ripple on oscillation in a non-mutually exclusive manner. Following the categorization, we removed residual ripple on spike events that had simultaneously occurred during oscillations. The accuracy of ripple classification was verified using ripple triggered averaging[27] (Supporting Information).

4.2. Calculation of ripple phasors occurring during sleep oscillations—To examine and quantify phase amplitude coupling, we transformed each ripple event into a ripple phasor, as described in Eqn. 2.,

$$ve^{i\theta}=\sum_{t}^{T}a\left(t\right)e^{i\phi(t)} \quad \text{Eqn. 2}$$

where v is the vector strength of the phasor, theta its phase angle, and a(t) and ø(t) are the respective instantaneous ripple amplitude and iEEG phase during the ripple across its duration [t.T] (Fig. 1).

ø(t) varied depending on whether the ripple was categorized as a ripple on slow wave, delta, theta, or spindle. For each band we calculated a unique instantaneous phase time series ø(t) using a Hilbert transform. Therefore, each ripple event superimposed on two or more, non-mutually exclusive oscillatory activities (e.g., slow and spindle band) resulted in a unique ripple phasor for each band.

5. Statistical analysis

5.1. Ripple phasor statistical methods—We developed a method to determine whether all the ripple phasors of a given type recorded from a single contact exhibited unimodal or bimodal clustering around preferred, i.e., mean phase angle(s). The clusters were subsequently used to separate the ripple phasors in to two distinct groups corresponding to those that occurred during the peak-trough and trough-peak transitions (Supplementary Fig. 1; Supporting information).

5.2 HFO-SOZ correlations—We used receiver operating characteristic (ROC) curves (Supporting Information), and a generalized estimated equation (GEE) approach (Supporting Information) to determine if different ripple types during sleep occurred more frequently inside than outside the SOZ.

Results

1. Patient characteristics and sleep recordings

We selected depth electrode intracranial EEG (iEEG) recordings from patients with focal-onset seizures. Nine patients had mesial temporal lobe epilepsy (MTLE; 7 unilateral, 2 bilateral), seven patients had mesial temporal and neocortical lobe epilepsy (MTLE+), and seven patients had neocortical epilepsy (NEO) (Supplementary Table 1). Among the 14 patients with neocortical SOZs, eight patients had SOZ sites located in the lateral temporal lobe, five patients had SOZ sites located in the frontal lobe, and six patients had SOZ sites located in the parietal lobe. We analyzed iEEG recordings ranging from between 7–17 depth electrodes with 7–16 contacts per patient (Supplementary Table 1).

2. Ripple oscillations superimposed on lower-frequency oscillations during sleep

We detected a total of 207,175 inter-ictal ripples, which occurred superimposed on either epileptiform spikes or normal sleep architecture (Fig. 2). The proportion of ripple events in each category is shown in Supplementary Table 2. Visual inspection of these ripples revealed that the ripple events could occur during diverse phases of the oscillations composing normal sleep architecture (Supplementary Fig. 2).

3. Association of ripple types with the seizure onset zone (SOZ) by neuroanatomical regions

To determine whether certain ripple types were generated at higher rates in epileptogenic regions, we generated receiver-operating characteristic (ROC) curves measuring the classification accuracy of ripple rates for the SOZ (Fig. 3). Overall, the rates of true ripples on spikes (AUC=0.78) were superior to those of ripples on oscillations (AUC=0.63 for ripples on spindle and theta; AUC=0.65 for ripples on delta and slow) for identifying frontal neocortical epileptogenic regions (all adjusted p=0.001). Mean rates of ripples on different oscillations were approximately equivalent with respect to localizing the SOZ. In a subset of patients with seizure free outcomes following surgery, we also compared the classification accuracy of each ripple type for resected regions, likely encompassing both epileptogenic and healthy tissue, and found no obvious difference between the subtypes of ripples on oscillations (Supplementary Fig. 3). The remainder of the analysis focused solely on the subtypes of ripples on oscillations, and ripple on spikes (true and false) were excluded.

4. Coupling between oscillatory phase and ripple event amplitude during sleep

We utilized ripple phasors that relate the phase of each lower-frequency oscillation to the amplitude of each ripple event (Fig. 4A–B; Supplementary Fig. 4A–B). As shown in Fig. 4C, polar plots of the population of delta ripple phasors identified in a single, neocortical depth electrode during the entire recording epoch often demonstrated two clusters of ripple phasor angles (i.e., a bimodal distribution). A bimodal distribution of ripple phasor angles recorded from a single macroelectrode was not only observed in the case of delta ripple phasors, but also for slow, theta, and spindle ripple phasors (Supplementary Table 2; Supplementary Fig. 4).

We next asked whether the preferred phase angle(s) of ripple coupling were consistent across multiple recording sites confined to an anatomical region (Supplementary Fig. 1). When we pooled all the mean phase angles across all the recording sites confined within each anatomical region, we found that the distribution of these mean phase angles was also bimodal (i.e., two distinct clusters). As shown in Fig. 4D and Supplementary Fig. 5, normalized polar plots of the mean phase angles showed that most ripple events occur during either the peak-trough or the trough-peak transition of slow, delta, theta, and spindle band activity (Kuiper's V-test, $p<0.05$). In the cases that the mean preferred phase angles occurred around the trough of an oscillation, these ripple events were labeled as the 'peak-trough transition', whereas if the preferred phase angles occurred during the peak of an oscillation, the events were labeled as the 'trough-peak transition' (Supplementary Table 5). Notably, the frequency of ripples occurring at a peak or trough and those during the

transition periods differed depending on neuroanatomical locations and sleep oscillatory types.

We next asked if ripple-triggered averaging (RTA) would also demonstrate bimodal phase-amplitude coupling similar to the ripple phasor analysis. The RTA results revealed that the modulating signal for ripples coupled to the peak-trough and trough-peak was significant and recapitulated the unique spectral feature of slow, delta, theta, and spindle band activity, which nested the ripple events (Fig. 5; Supplementary Fig. 6). The modulating signal for ripples occurring during the peak-trough transition of theta and spindle band activity exhibited a morphology superimposed by a slow wave, which may correspond to the "down-up transition", as described in the previous literature[24] (Supplementary Fig. 7). In contrast, the modulating signal for the ripples occurring during the trough-peak transition of theta and spindle failed to exhibit a superimposed slow wave, which may correspond to the "up-down transition". However, the reversed polarity of the depth iEEG and scalp potentials was only available from limited neuroanatomical regions in few patients. Thus, it is inconclusive whether or not the depth iEEG polarity reflects the up and down state of a slow wave from the reference point of scalp recordings.

5. Distinct couplings between sleep oscillatory phase and ripple event amplitude in and outside the SOZ

We asked if the preferred phase angle of coupling between oscillatory phase and ripple event amplitude during sleep differed in the SOZ as compared with the NSOZ. In the absence of an *a priori* assumption regarding the distribution of ripple phasor angles, we still observed differences between phase-event amplitude coupling in the SOZ and NSOZ. In the parietal lobe (Fig. 6A), there was a statistically significant difference in the distribution of ripple phasor angles detected in the SOZ as compared with the NSOZ for all oscillatory types coupled with ripple events. The distinction was strongest for ripples on delta ($k = 1.71E+06$, $p=0.001$). We also observed statistical differences for other ripple types in other neuroanatomical locations (Supplementary Fig. 8). Although the Kuiper's tests do not specify which properties of two raw circular data differ from one another, our finding as shown in Fig. 6B–C suggests that the mean location of the preferred phase angles of ripple-slower oscillation coupling differ significantly in the SOZ relative to NSOZ.

When it was assumed that ripple event amplitude could be coupled with oscillatory phase around two preferred phase angles (i.e., two clusters), the relationship between the preferred phase of ripple coupling and the location of the SOZ could be better quantified (Fig. 6B–C). The incidence ratio of ripples occurring during the peak-trough transition of slow oscillations was not significant in the parietal lobe ($p=0.494$), or did not reach significance in the frontal lobe after correction for multiple comparisons ($p=0.024$). However, the incidence ratio of ripples occurring during the trough-peak transition of slow oscillations was significant in both the parietal ($p=0.001$) and frontal lobe SOZ ($p=0.004$). The effect size was larger in the parietal lobe as compared with the frontal lobe. We observed a similar distinction for ripples occurring during the peak-trough and trough-peak transition of delta and theta band activity in the parietal lobe. In the frontal lobe, the incidence ratio of ripples occurring during the peak-trough ($p=0.002$) and trough-peak transition ($p=0.019$) were both

significant, but for theta (p=0.006) and spindle (p=0.009) ripples only the incidence ratio of ripples occurring during the trough-peak transition was significant. In frontal and parietal lobe SOZ, the increased incidence ratio of ripples occurring during the trough-peak transition of oscillations was observed from a majority of patients, and also in the resected region for two patients with neocortical epilepsy, who were seizure free following surgery (Supplementary Fig. 9). Neither cluster of ripple phasors was increased in rates selectively for the SOZ located within the lateral temporal lobe (all $p > 0.09$), whereas both clusters of ripple phasors were increased in rates in the mesial temporal SOZ relative to NSOZ (all $p < 0.005$).

We also asked if contacts in SOZ sites more often exhibited a bimodal distribution (i.e., two clusters) of preferred ripple phasor angles, as compared with contacts in NSOZ sites. We found that in the parietal lobe, and to a lesser extent the frontal lobe, a greater proportion of recording sites in the SOZ exhibited a bimodal as opposed to a unimodal distribution (i.e., one cluster) of ripple phasor angles (Supplementary Table 6).

Discussion

We report that in single macroelectrode recording sites in patients with medically-refractory focal epilepsy, coupling between oscillatory phase and ripple event amplitude could occur at either one or two distinct preferred phase angles for slow, delta, theta, and spindle band activity. Across multiple recording sites, confined within each lobe (i.e., frontal, parietal, lateral temporal, and mesial temporal), the mean phase angles of coupling were relatively consistent and exhibited bimodality (i.e., two clusters). Using these two clusters of ripple phasors to distinguish the ripple events occurring at distinct phases of slower sleep oscillations, we found that the SOZ incidence ratio for ripples occurring during the trough-peak transition of oscillations was selectively elevated in the frontal and parietal lobe.

Differences between ripple types and subtypes

True and false ripple on spike rates trended towards providing superior classification accuracy compared to ripple on oscillation rates across neuroanatomical regions. False ripple on spikes result from ripple-frequency filter ringing from sharply contoured inter-ictal discharges. Thus, false ripples on spikes are not generated by all epileptiform discharges, and may reflect only the discharges produced by action potentials, i.e., synchronized population spikes[25]. The inferiority of ripples on oscillations suggests that at least a portion of these events may be physiological as opposed to pathological[5], thus necessitating further analysis to provide better classification accuracy.

Sleep oscillatory phase and ripple event amplitude are coupled at one or two distinct phase angles

We observed that ripples mostly occurred during either the peak-trough or trough-peak transition of slower oscillations, and near the peak or trough of faster oscillations. These ripple events occurred primarily during one of the transitions at certain recording sites, whereas at other recording sites a substantial proportion of ripples occurred during both transitions.

Under a variety of experimental conditions during wakefulness the phase of a slower frequency can be coupled with the amplitude of a faster frequency at a single preferred phase angle. This form of coupling mediates active perception and cognition by potentially binding together anatomically-dispersed functional cell assemblies[26]. The phase-event amplitude coupling between ripples and sleep oscillations seen in patients with focal seizures is unique because it can occur at two preferred phase angles.

In patients with focal seizures, ripples occur on slow waves during the transition from the down-up and up-down state[5,17]. We replicated these results, but since we measured the slow wave using depth iEEG we found that putative pathological ripples in the cortex occurred during the trough-peak transition (Supplementary Fig. 6). In the mesial temporal lobe, the phase relationship between potentials recorded from depth electrodes and the scalp may be more complex[11].

The mechanisms that generate ripples during the down-up transition are likely distinct from those that generate ripples during the up-down transition. The down-up transition is mediated by the synchronous summation of miniature EPSPs promoted by the involvement of an active inhibitory circuit of cortical interneurons[7]. The up-down transition is mediated primarily by inhibitory interneurons that act to synchronously hyperpolarize relatively large neuronal networks and disfacilitation[27].

During sleep, in healthy primates, hippocampal ripples occur mostly during the down-up transition phase of the hippocampal delta oscillation[28]. Mechanisms that generate delta oscillations may be distinct from slow oscillations[6], but the differences have yet to be clearly defined. We observed that in patients with epilepsy ripple amplitude could be coupled to the delta phase at two preferred phase angles.

Theta-ripple coupling during sleep has been reported in the literature of both REM and NREM sleep. Theta oscillations are considered to be volume-conducted from the mesial temporal regions during wakefulness[29] and REM sleep[30,31]. Since our customized algorithm allowed for different frequency bursts of oscillations to be identified during a single ripple event, we found that most ripple events classified as those superimposed on theta frequency activity (4–10Hz) were also classified as those superimposed on spindle frequency activity (12–16 Hz). Therefore, theta-band activity coupled with ripples observed in our present study may reflect the spectral properties of slow spindles (9–12 Hz)[32].

Coupling between ripple events and spindle activity at a preferred phase angle of the trough was observed from juxtacellular recordings of healthy rodent neocortex (layer II/III), which may mediate the information transfer via hippocampal-cortical and intra-cortical communications[15]. In patients with epilepsy, we observed that ripple amplitude was coupled not only to the trough, but to the peak of spindle band oscillations.

Nested oscillations during sleep modulate ripple amplitude during a slow wave down-up transition

In wide-bandwidth iEEG recordings, we found that ripple events often occurred on oscillatory bursts with diverse frequency content. By allowing each ripple event to be

classified in to non-mutually exclusive oscillation types, we could evaluate the relationship between co-occurring or nested oscillatory events using the ripple-triggered averaging method. The modulating signals from this approach revealed that the ripple events that reached maximum amplitude during the peak-trough transition (or trough) of theta- and spindle-band oscillations were also modulated by the phase of slow oscillations (Fig. 5; Supplementary Fig. 6). Based on limited evidence of the reversed polarity of depth iEEG and scalp potentials (Supplementary Fig. 7), our results suggest that the preferred phase angle of a slow wave coupled with faster oscillations and ripple events may correspond to its down-up transition. The relationship between the polarity of iEEG and scalp EEG recordings are likely more complex, and future work is required to related local slow wave to global slow wave activity. This hierarchy of nested oscillations consisting of ripple band, spindle band, and slow oscillations was seen in both neocortical and mesial-temporal recording sites. In contrast, the modulating signal of ripples occurring during the trough-peak transition (or peak) of theta and spindle-band activity did not exhibit coupling to the trough-peak transition of a superimposed slow wave. A similar hierarchy of nested oscillations occurring during the down-up transition was identified in previous iEEG studies from human hippocampus[13,14].

Preferred phase angles of ripples coupled with sleep oscillations may be distinct in the frontal and parietal SOZ

In all brain regions, including non-epileptogenic sites, we observed bimodal phase-amplitude coupling at a group level. However, in epileptogenic sites in the frontal and parietal lobe bimodal phase-amplitude coupling was present more often in single contacts of the SOZ. In accord with prior published work[5,17], the rates of ripples occurring at the trough-peak transition of slow waves (i.e., up- down transition) were increased in macroelectrodes located in the frontal and parietal lobe SOZ, relative to electrodes located in the frontal and parietal NSOZ. In contrast, the rates of ripples occurring at the peak-trough (i.e., down- up) transition were not increased in these same SOZs. Therefore, the preferred phase angle of coupling between ripples and slow waves can help distinguish putative pathological from physiological events in the frontal or parietal lobe.

The mechanisms that increase coupling between ripples and slow oscillations at the preferred phase angle of the trough-peak transition in the frontal and parietal SOZ remain unclear. Global sleep slow waves occur first in the frontal lobe and propagate quickly to the parietal lobe, but with a longer latency to lateral and mesial temporal regions[10]. Larger slow waves could drive pathological ripples and seizures in patients with frontal and parietal lobe focal epilepsy that have nocturnal seizures[2]. Paroxysmal activity may selectively occur during the trough-peak (up-down) transition due to disfacilitation[27,33,34] and synaptic inhibition promoting excitation in a paradoxical fashion[35–37].

The hitherto unresolved relationship between delta, theta, and spindle-band phase, ripple amplitude, and the location of the seizure onset zone suggests that mechanistic differences driven by the peak-trough and trough-peak transitions of these oscillations can also drive the generation of putative physiological and pathological ripples, respectively. For patients with a parietal lobe SOZ, ripples coupled with the trough-peak transition of delta and theta waves

were generated primarily in epileptogenic regions. For patients with a frontal lobe SOZ, ripples coupled with the trough-peak (or peak) of theta and spindle-band oscillations were generated primarily in epileptogenic regions. Prior studies have suggested that ripples occurring at the trough of spindle oscillations are predominantly physiological[13,14].

Study limitations

One limitation of our study is that, due to lack of EMG/EOG availability, we could not stage early/late NREM and REM sleep. By classifying sleep architecture using an amplitude based criteria, we were able to recognize epochs of high amplitude slow and delta activity that can stage sleep even in the absence of EMG/EOG[19].

It is also premature to conclude that ripple events that are coupled to phase angles distributed within the peak-trough transition of slower oscillations are physiological[18,38,39], whereas those distributed within the trough-peak transition are pathological. Moreover, SOZ incidence ratios of ripple coupling at both phase angles of slower oscillations were increased in mesial temporal recording sites. Future studies should utilize behavioral paradigms and post-operative seizure outcome data in better differentiating physiological and and pathological ripples.

Conclusions

We found that putative physiological and pathological ripples could be distinguished during sleep in the frontal and parietal lobes on the basis of the preferred angle of coupling between slow, delta, theta, and spindle-band oscillatory phase and ripple amplitude. Utilizing the two distinct preferred phase angles of coupling during sleep may help delineate the epileptic network activity for patients with frontal and parietal lobe focal seizures.

Supplementary Material

Refer to Web version on PubMed Central for supplementary material.

Acknowledgments

This work was supported by a grant from the National Institutes of Health K23 NS094633-01A1 to Dr. Shennan A. Weiss.

The authors are grateful to Dr. John Stern, Dr. Dawn Eliashiv, Dr. Scott Mintzer, Dr. Maromi Nei, and Dr. Christopher Skidmore for clinical support; Mr. Dale Wyeth, Mr. Edmund Wyeth, and Dr. Shoichi Shimamoto for technical support.

References

1. Kataria L, Vaughn BV. Sleep and Epilepsy. Sleep Med Clin. 2016; 11:25–38. [PubMed: 26972031]
2. Herman ST, Walczak TS, Bazil CW. Distribution of partial seizures during the sleep–wake cycle: differences by seizure onset site. Neurology. 2001; 56:1453–1459. [PubMed: 11402100]
3. Loddenkemper T, Vendrame M, Zarowski M, et al. Circadian patterns of pediatric seizures. Neurology. 2011; 76:145–153. [PubMed: 21220719]
4. Nobili L, Francione S, Mai R, et al. Surgical treatment of drug-resistant nocturnal frontal lobe epilepsy. Brain. 2007; 130:561–573. [PubMed: 17124189]

5. Frauscher B, von Ellenrieder N, Ferrari-Marinho T, et al. Facilitation of epileptic activity during sleep is mediated by high amplitude slow waves. Brain. 2015; 138:1629–1641. [PubMed: 25792528]
6. Buzsáki, G. Rhythms of the brain. Oxford University Press; 2006.
7. Timofeev IV. Neuronal plasticity and thalamocortical sleep and waking oscillations. Prog Brain Res. 2011; 193:121–144. [PubMed: 21854960]
8. Amzica F, Steriade M. Short- and long-range neuronal synchronization of the slow (< 1 Hz) cortical oscillation. J Neurophysiol. 1995; 73:20–38. [PubMed: 7714565]
9. Steriade M, Contreras D, Curró Dossi R, et al. The slow (< 1 Hz) oscillation in reticular thalamic and thalamocortical neurons: scenario of sleep rhythm generation in interacting thalamic and neocortical networks. J Neurosci. 1993; 13:3284–3299. [PubMed: 8340808]
10. Nir Y, Staba RJ, Andrillon T, et al. Regional slow waves and spindles in human sleep. Neuron. 2011; 70:153–169. [PubMed: 21482364]
11. Grenier F, Timofeev IV, Steriade M. Focal synchronization of ripples (80–200 Hz) in neocortex and their neuronal correlates. J Neurophysiol. 2001; 86:1884–1898. [PubMed: 11600648]
12. Grenier F, Timofeev IV, Steriade M. Neocortical very fast oscillations (ripples, 80–200 Hz) during seizures: intracellular correlates. J Neurophysiol. 2003; 89:841–852. [PubMed: 12574462]
13. Clemens Z, Mölle M, Eross L, et al. Temporal coupling of parahippocampal ripples, sleep spindles and slow oscillations in humans. Brain. 2007; 130:2868–2878. [PubMed: 17615093]
14. Staresina BP, Bergmann TO, Bonnefond M, et al. Hierarchical nesting of slow oscillations, spindles and ripples in the human hippocampus during sleep. Nat Neurosci. 2015; 18:1679–1686. [PubMed: 26389842]
15. Averkin RG, Szemenyei V, Bordé S, et al. Identified Cellular Correlates of Neocortical Ripple and High-Gamma Oscillations during Spindles of Natural Sleep. Neuron. 2016; 92:916–928. [PubMed: 27746131]
16. Jacobs J, LeVan P, Chander R, et al. Interictal high-frequency oscillations (80–500 Hz) are an indicator of seizure onset areas independent of spikes in the human epileptic brain. Epilepsia. 2008; 49:1893–1907. [PubMed: 18479382]
17. von Ellenrieder N, Frauscher B, Dubeau F, et al. Interaction with slow waves during sleep improves discrimination of physiologic and pathologic high-frequency oscillations (80–500 Hz). Epilepsia. 2016; 57:869–878. [PubMed: 27184021]
18. Axmacher N, Elger CE, Fell J. Ripples in the medial temporal lobe are relevant for human memory consolidation. Brain. 2008; 131:1806–1817. [PubMed: 18503077]
19. Kremen V, Duque JJ, Brinkmann BH, et al. Behavioral state classification in epileptic brain using intracranial electrophysiology. J Neural Eng. 2017; 14:026001. [PubMed: 28050973]
20. Weiss SA, Orosz I, Salamon N, et al. Ripples on spikes show increased phase-amplitude coupling in mesial temporal lobe epilepsy seizure-onset zones. Epilepsia. 2016; 57:1916–1930. [PubMed: 27723936]
21. Shimamoto S, Waldman Z, Orosz I, et al. Utilization of independent component analysis for accurate pathological ripple detection in intracranial EEG recordings recorded extra- and intra-operatively. Submitted.
22. Bénar CG, Chauvière L, Bartolomei F, et al. Pitfalls of high-pass filtering for detecting epileptic oscillations: a technical note on “false” ripples. Clin Neurophysiol. 2010; 121:301–310. [PubMed: 19955019]
23. Waldman Z, Song I, Oroz I, et al. A method for the topographical identification and quantification of high frequency oscillations in intracranial electroencephalography. Submitted.
24. Steriade M. Grouping of brain rhythms in corticothalamic systems. Neuroscience. 2006; 137:1087–1106. [PubMed: 16343791]
25. Bragin A, Csicsvári J, Penttonen M, et al. Epileptic afterdischarge in the hippocampal-entorhinal system: current source density and unit studies. Neuroscience. 1997; 76:1187–1203. [PubMed: 9027878]
26. Canolty RT, Knight RT. The functional role of cross-frequency coupling. Trends Cogn Sci. 2010; 14:506–515. [PubMed: 20932795]

27. Timofeev IV, Grenier F, Steriade M. Disfacilitation and active inhibition in the neocortex during the natural sleep-wake cycle: an intracellular study. Proc Natl Acad Sci U S A. 2001; 98:1924–1929. [PubMed: 11172052]
28. Logothetis NK, Eschenko O, Murayama Y, et al. Hippocampal-cortical interaction during periods of subcortical silence. Nature. 2012; 491:547–553. [PubMed: 23172213]
29. Kahana MJ, Seelig D, Madsen JR. Theta returns. Curr Opin Neurobiol. 2001; 11:739–744. [PubMed: 11741027]
30. Sirota A, Montgomery S, Fujisawa S, et al. Entrainment of neocortical neurons and gamma oscillations by the hippocampal theta rhythm. Neuron. 2008; 60:683–697. [PubMed: 19038224]
31. Scheffzük C, Kukushka VI, Vyssotski AL, et al. Selective coupling between theta phase and neocortical fast gamma oscillations during REM-sleep in mice. PLoS One. 2011; 6:e28489. [PubMed: 22163023]
32. Rasch B, Born J. About sleep's role in memory. Physiol Rev. 2013; 93:681–766. [PubMed: 23589831]
33. Timofeev IV, Taranenko VD. Changes in the responsive ability of parietal associative cortex neurons to stimulation of associative thalamic nuclei during development of inhibition. Neirofiziologiia. 1992; 24:198–207. [PubMed: 1598124]
34. Timofeev IV, Bazhenov M, Sejnowski T, et al. Cortical hyperpolarization-activated depolarizing current takes part in the generation of focal paroxysmal activities. Proc Natl Acad Sci U S A. 2002; 99:9533–9537. [PubMed: 12089324]
35. Klaassen A, Glykys J, Maguire J, et al. Seizures and enhanced cortical GABAergic inhibition in two mouse models of human autosomal dominant nocturnal frontal lobe epilepsy. Proc Natl Acad Sci U S A. 2006; 103:19152–19157. [PubMed: 17146052]
36. Mann EO, Mody I. The multifaceted role of inhibition in epilepsy: seizure-genesis through excessive GABAergic inhibition in autosomal dominant nocturnal frontal lobe epilepsy. Curr Opin Neurol. 2008; 21:155–160. [PubMed: 18317273]
37. Bragin A, Benassi SK, Engel J. Patterns of the UP-Down state in normal and epileptic mice. Neuroscience. 2012; 225:76–87. [PubMed: 22960310]
38. Mölle M, Born J. Slow oscillations orchestrating fast oscillations and memory consolidation. Prog Brain Res. 2011; 193:93–110. [PubMed: 21854958]
39. Feld GB, Born J. Sculpting memory during sleep: concurrent consolidation and forgetting. Curr Opin Neurobiol. 2017; 44:20–27. [PubMed: 28278432]

Key Point Box

- In patients with focal seizures, coupling between ripple amplitude and sleep oscillatory phase occurs at two clusters of phase angles.
- The preferred phase angles of coupling are consistent across individual sites within neuroanatomical regions.
- The preferred phase angles of coupling for ripples observed with the seizure onset zone (SOZ) are distinct from the non-SOZ (NSOZ).
- Ripples that occur during the intracranial EEG trough-peak transition (or peak) of oscillations occur relatively more often in the SOZ.
- For patients with frontal and parietal focal seizures, the preferred phase angle of ripple coupling with sleep oscillations can be informative to identify regions with epileptic activity.

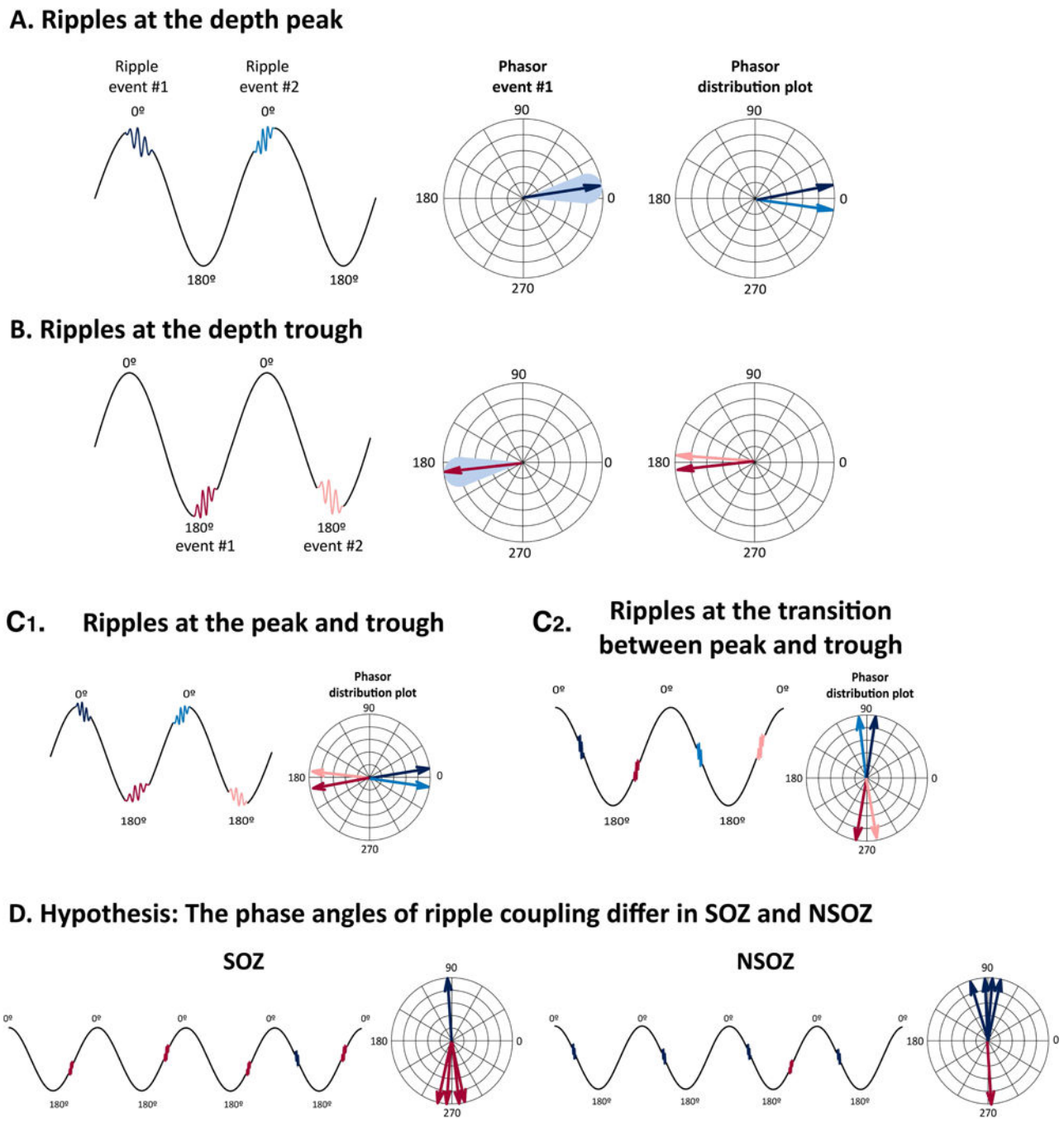

Figure 1. Illustration of the phase angles of oscillations coupled with ripple events during sleep

(A) Phasor derivation of a ripple event occurring at the peak of the oscillation and phasor distribution plot of two events. An individual phasor of the ripple event #1 (blue arrow) is derived from the instantaneous phase of the sinusoidal wave and the instantaneous amplitude in the ripple band (80–150 Hz) during the duration of the event (areas shaded in gray). The phasor distribution plot shows the two derived ripple phasors occurring at the peak of the sinusoidal wave. (B) Phasor derivation of a ripple event occurring at the trough of the oscillation and the corresponding phasor distribution plot for the two events. (C_1) Each

phasor is derived from each ripple event occurring either at the peak (blue and light blue) or at the trough (red and pink) of a sinusoidal wave. (C_2) Each phasor is derived from each ripple event occurring during the peak-trough transition *i.e.* slow wave depth iEEG down-up (blue and light blue) or at the trough-peak transition *i.e.* slow wave depth iEEG up-down (red and pink) of a sinusoidal wave. (D) The study hypothesis illustrated by simulated ripple events occurring at different phase angles of oscillations in the SOZ and the non-SOZ (NSOZ).

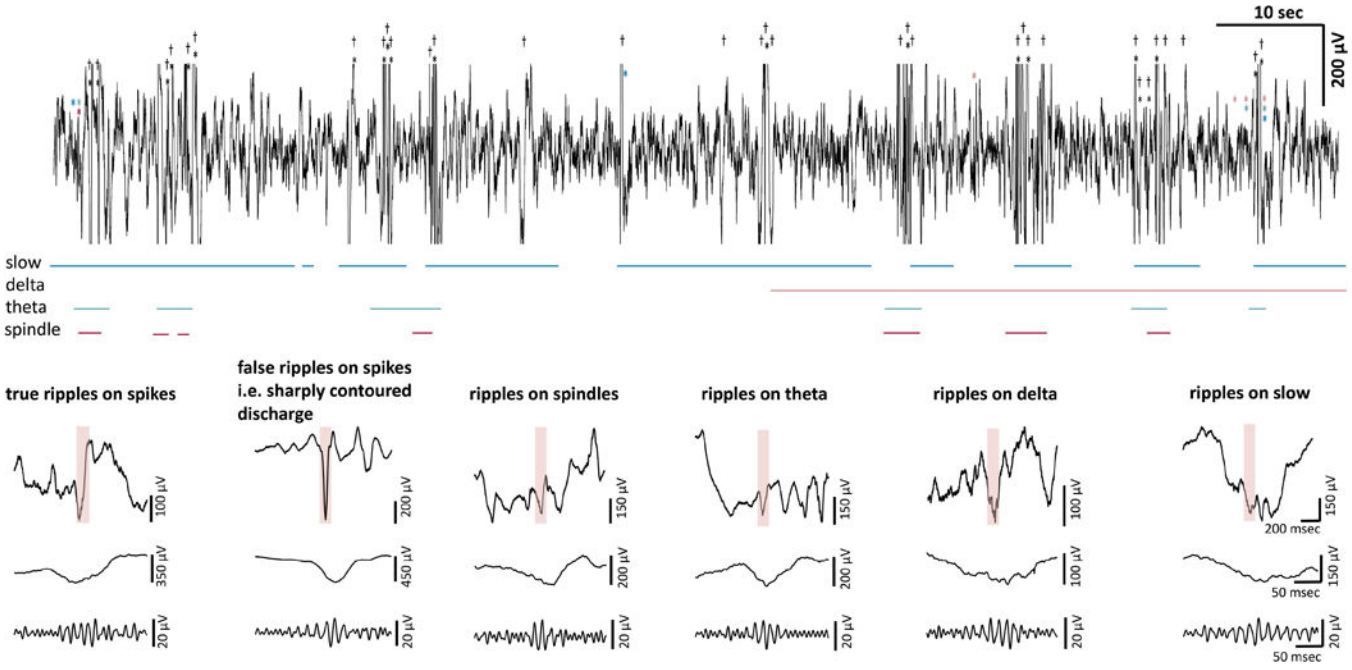

Figure 2. A taxonomy of ripples on interictal spikes and oscillations during sleep

(A) A 2-minute raw intracranial EEG (iEEG) illustrating distinct ripple types and ripple events on non-mutually exclusive oscillations during sleep. (B) Examples of unfiltered raw iEEG (top trace), expanded raw iEEG (middle trace, pink), and filtered ripples (80–150 Hz; bottom trace) of true ripples on spikes, false ripples on spikes, i.e., sharply contoured spikes that result in ripple frequency filter ringing, ripples on spindle (12–16 Hz), ripples on theta (4–10 Hz), ripples on delta (2–4 Hz), and ripples on slow band activity (0.1–2 Hz). Ripple events are denoted by asterisks (*) and interictal spikes are denoted by obelisks (†).

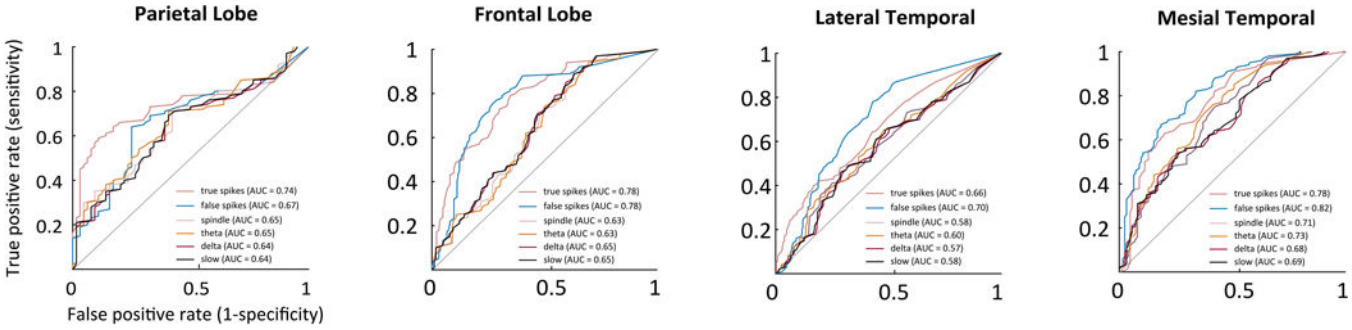

Figure 3. Receiver operating characteristic (ROC) curves and corresponding area under the curve (AUC) statistics for predicting SOZ by ripples on interictal spikes and sleep oscillations in neocortical and mesial temporal lobes

Compared to ripples on oscillations, both true and false ripples on spikes better predicted the SOZ across neuroanatomical structures. The accuracy of ripples on sleep oscillations was similar across distinct frequency band activities with which ripples occurred ($p \geq 0.05$).

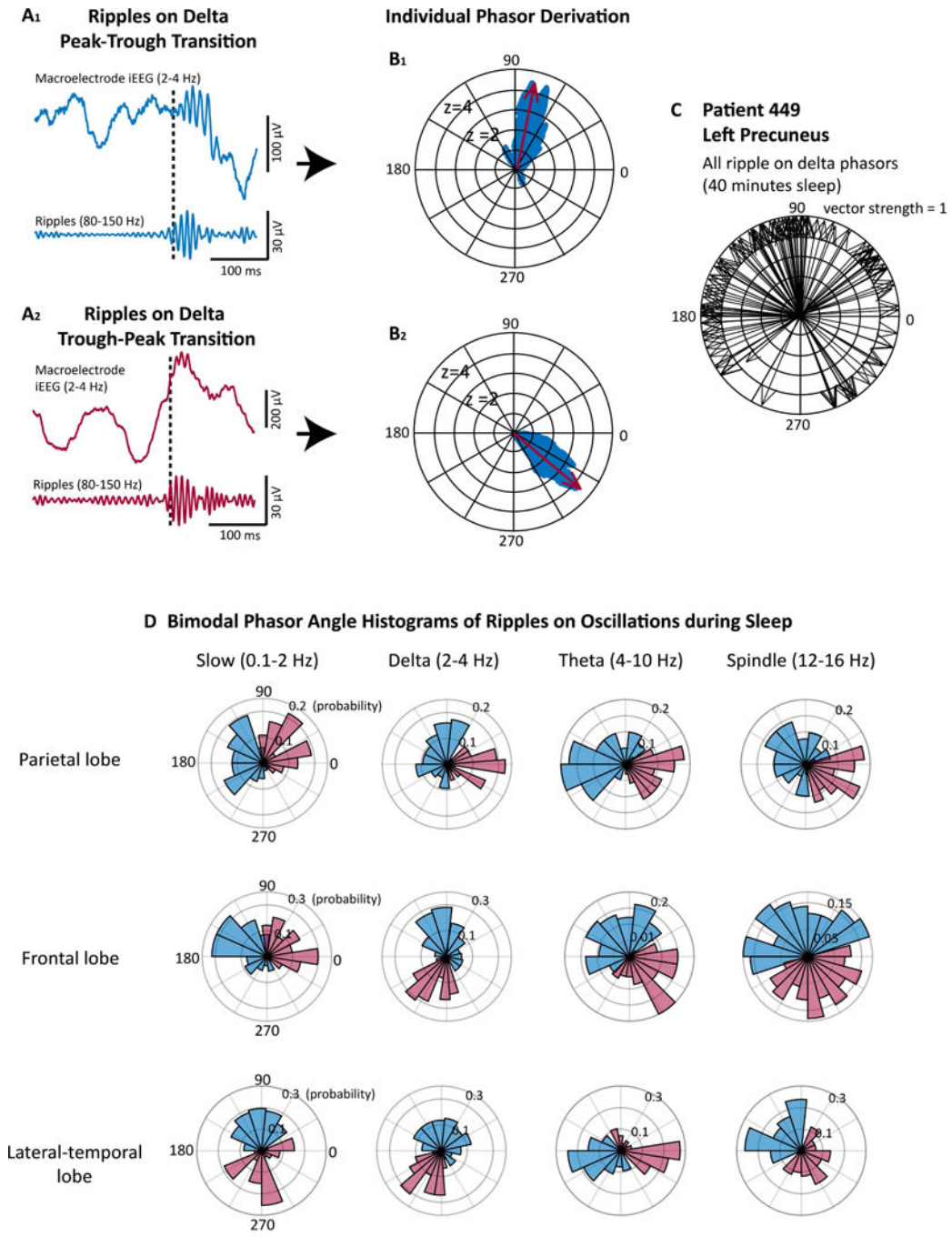

Figure 4. Bimodal coupling between oscillation phase and ripple event amplitude using ripple phasors

(A) Ripples occurring during the transition phase of the depth iEEG peak-trough (A_1) and the trough-peak (A_2) of 2–4 Hz delta band activity from unfiltered (top trace) and band-pass (80–150 Hz, bottom trace) iEEG. (B) Description of individual phasor derivation from A_1 and A_2. Phase angles of delta band activity coupled with each ripple event are denoted by blue arrows and the preferred phase angle of the phasor and vector strength is shown in red arrow. (C) Two clusters of ripple phasor angles (i.e., bimodal phase-event amplitude coupling) are evident in the population of delta ripple phasors isolated from a single

macroelectrode during a 40-minute sleep recording from the left precuneus in a patient with a parietal SOZ. (D) Normalized rose (i.e., circular) histograms of the mean preferred phase angle across all patients and electrodes in parietal (top), frontal (middle), and lateral temporal regions (bottom). Blue denotes the phase distribution for ripple events occurring during the depth iEEG peak-trough transition (or at the trough), and red denotes those occurring during the trough-peak transition (or at the peak).

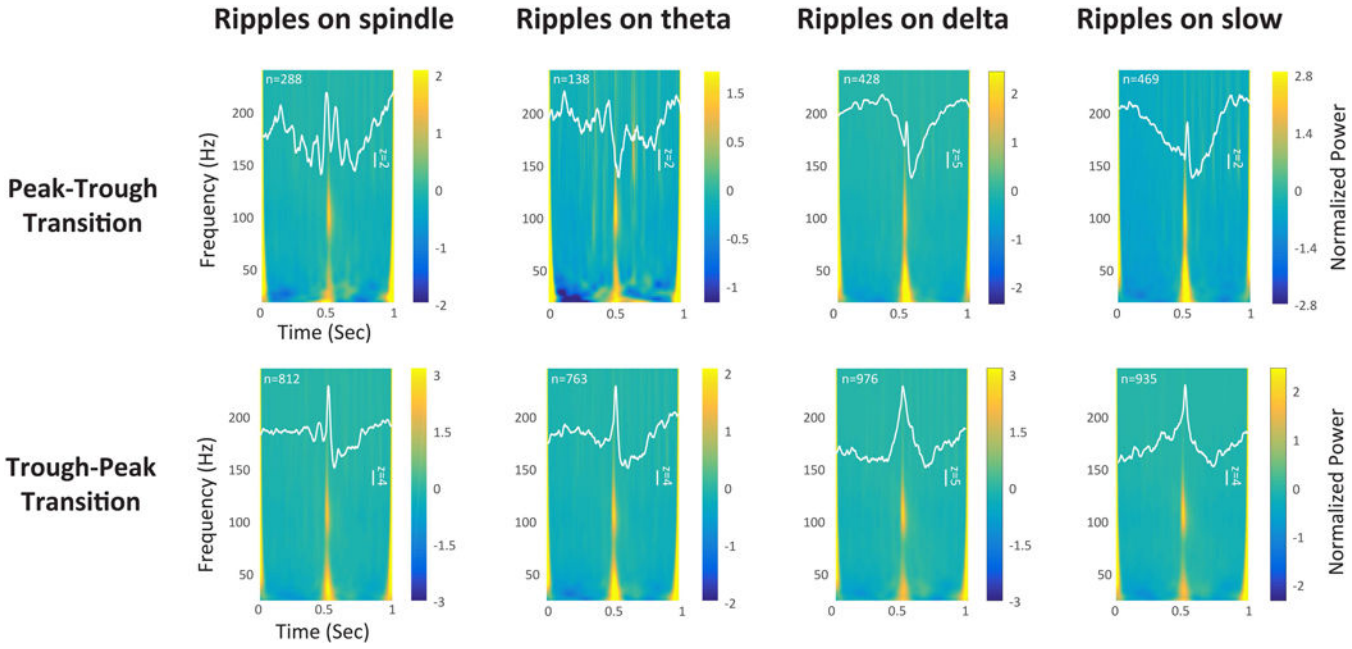

Figure 5. Bimodal phase-event amplitude coupling of ripples and sleep oscillations by ripple-triggered averaging in a patient with neocortical seizure onset

The ripple-triggered average of all ripple phasors occurring during the depth iEEG peak-trough transition (or at the trough) and the trough-peak transition (or at the peak) of sleep oscillations from a patient with the parietal lobe SOZ demonstrates that ripple event amplitude is modulated by a signal that recapitulates the underlying spectral features of the ripple taxonomy. The resulting ripple-triggered averaged waveform (modulating signal, white trace) had a peak-to-peak amplitude corresponding to the strength of coupling and a phase at time 0.5 sec corresponding to the preferred phase of coupling. The superimposed normalized averaged time-frequency representation of the aligned unfiltered ripple events was calculated by wavelet convolution. The modulating signal for ripples occurring during the peak-trough transition (or at the trough) of spindles and theta band activity exhibited a superimposed down-up transition of a slow wave. The modulating signals also exhibited sharp transients coinciding with the ripple event, and the modulating signal for trough-peak ripples on theta and spindles failed to exhibit clear oscillatory components. The number of 1 sec iEEG traces used to derive the ripple-triggered averaging is denoted as ‘n’ at the left top corner of each image.

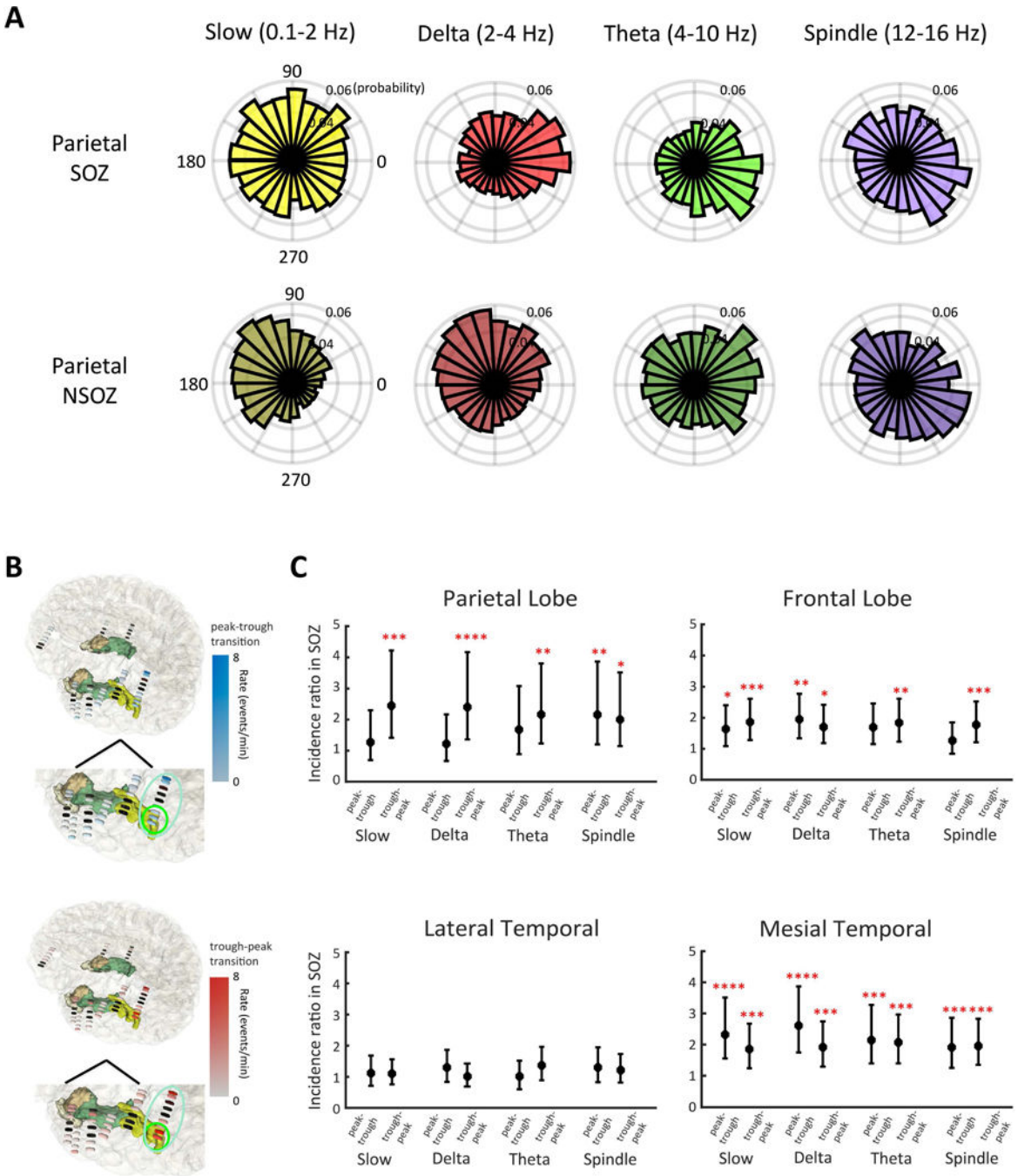

Figure 6. Distinction of the SOZ and NSOZ in patients with neocortical epilepsy based on the bimodal phase-amplitude coupling of ripple events occurring with oscillations during sleep

(A) Normalized rose (i.e., polar) histograms of the preferred phase angle of all ripple phasors pooled across all patients and all recording sites in the parietal lobe SOZ and NSOZ, showing differences in the preferred phase angle of coupling between ripples and sleep slower oscillations. (B) A reconstructed image of patient 2 (449) and the rates (events/min) of ripples on delta occurring during the depth iEEG peak-trough transition (top) and the trough-peak transition (bottom) from a patient with parietal seizure onset. (C) Incidence

ratio of ripples occurring during the depth iEEG peak-trough transition (or at the trough) and the trough-peak transition (or at the peak) of slow, delta, theta, and spindle band activity in the SOZ relative to the NSOZ in the parietal, frontal, lateral temporal, and mesial-temporal structures.